Nigerian Journal of Technology (NIJOTECH)
Vol. 43, No. 4, December, 2024, pp.795 - 806
www.nijotech.com

Print ISSN: 0331-8443
Electronic ISSN: 2467-8821
https://doi.org/10.4314/njt.v43i4.20

EFFECT OF CRITICAL BATCH VARIABLES ON THE EFFICIENCY AND KINETICS OF ADSORPTION OF NI (II) ONTO CARBONIZED AND UNCARBONIZED PALM KERNEL CHAFF

AUTHORS:
C. C. Nnaji[1,2] and A. Agim[3]

AFFILIATIONS:
[1]Department of Civil Engineering, University of Nigeria, Nsukka.
[2]Faculty of Engineering and Built Environment, University of Johannesburg, South Africa.
[3]School of Engineering and Computing, University of Huddersfield, Huddersfield, UK

***CORRESPONDING AUTHOR:**
Email: Akambende.agim@hud.ac.uk

ARTICLE HISTORY:
Received: 20 June, 2024.
Revised: 23 November, 2024.
Accepted: 28 November, 2024.
Published: 31 December, 2024.

KEYWORDS:
Absorption, Palm kernel chaff, Water treatment, Biosorbent.

ARTICLE INCLUDES:
Peer review

DATA AVAILABILITY:
On request from author(s)

EDITORS:
Ozoemena Anthony Ani

FUNDING:
None

Abstract

A series of batch experiments were conducted for refined CPKC (carbonized sample) and UCPKC (uncarbonized sample) using 10, 30, 50, 70, 100 and 120 mg/L of Ni (II) solution at 30°C, 35°C and 40°C at pH 3 and pH 9. Adsorption kinetics were investigated by determining the concentration of Ni (II) removed by the adsorbent at precise moments of time of 5, 10, 20, 30, 40, 60, 90 and 120 minutes. Standard kinetic equations were used to model data obtained from the experiments. For the range of conditions studied, the best improvement in the rate of adsorption and the adsorption capacity was observed for the carbonized sample at a temperature of 35°C. The rate constants of PKC were notably higher in an alkaline solution when the initial pH at the start of mixing was measured at 9, compared to the acidic solution with an initial pH of 3, across all studied temperatures. The rate constants of PSO_1, PSO_2, PSO_3, PSO_4, PSO_5 and PSO_6 for CPKC ranged from 0.06 – 0.16, 0.14 – 0.44, 0.13 – 0.42, 0.13 – 0.30 and 0.09 – 0.59 g/mg.min^{-1}. In nearly all cases, PSO_1 model showed better correlation than other kinetic models with R^2 values ranging from 0.8 to 1.0. The average increase in adsorption rate constant for CPKC (pH 3), CPKC (pH 9), UCPKC (pH 3) and UCPKC (9) for 1°C increase in temperature was 0.31, 0.98, 0.51 and 0.43 mg/g.min respectively. The kinetic models were ranked as follows: /PSO_1/>/PFO/>/PSO_{2-5}/>/PSO_6/.

1.0 INTRODUCTION

Nickel, a naturally occurring white ferromagnetic metal is largely present in the environment. In natural water bodies, the metal is present in the form of the ion, nickel hexahydrate $\left[Ni(H_2O)_6{}^{2+}\right]$ [1], [2]. The best pH for this natural occurrence is 5 – 9 where complex ligands may be formed. However, acute exposure to this substance exceeding the normal concentration limit in water of 80µg/L has been shown by extensive evidence to have significant impacts on both human and animal health. The main reported effects of excessive nickel exposure for humans are gastrointestinal, neurological, and skin ailments. Genchi et al [3] argued that nickel (II) exposure induces mitochondrial damage, DNA hypermethylation, and histone modification which exacerbates oxidative stress and creates conditions for carcinogenesis.

Despite the deleterious effects of nickel, the metal is vital in metallurgy to produce metal alloys used for engines, turbine blades, domestic appliances made of

HOW TO CITE:
Nnaji, C. C., and Agim, A. "Effect of Critical Batch Variables on the Efficiency and Kinetics of Adsorption of Ni (II) onto Carbonized and Uncarbonized Palm Kernel Chaff", *Nigerian Journal of Technology*, 2024; 43(4), pp. 795 – 806; *https://doi.org/10.4314/njt.v43i4.20*

stainless steel, and electric vehicles. In the crude oil refining industry, catalysts necessary for chemical process have nickel additives which makes the metal indispensable [4]. Considering these benefits therefore, the challenge for scientist and engineers is to develop novel remedial methods for heavy nickel contamination in drinking water to mitigate the negative health effects on human and animal life. Over the years, the adsorption process has gained prominence in the removal of metallic ions from water. Usually, an attempt is made to alter or improve targeted physicochemical properties of the adsorbent such as pH, concentration, temperature and incident time as well as the sorption process to transform the surface of the adsorbent and improve the level of remediation achieved [5], [6]. Several studies have demonstrated that various forms of organic materials with favourable surface characteristics can adsorb and retain large amounts of contaminants. Good adsorbent-adsorbate results have been reported by various researchers for copper using *Rosa damascene* leaf power [7], highly toxic industrial dyes such as Acid Yellow, Congo Red, Methylene Blue, cationic and anionic dyes using activated carbon products from industrial and biomass wastes with maximum sorption of up to 769.23 mg/g [8], [9], [10], [11]; non-biodegradable carcinogenic methylene blue dye using Pseudomonas Alcaliphila and Rumex Abyssinicus Plant biosorbents [12], [13] and Potassium permanganate dye using Foeniculum vulgare seeds powder [14]. Also, biosorbents made from Zirconia Nano Fibers, Immobilised Archaeal Cells and Michelia figo sawdust were recorded to possess active sites for the extraction of heavy elements such as Chromium, Cadmium, Copper, and Lead. Regarding Nickel (II) specifically, chemically modified peanut husk powder and Lichen (*Parmotrema tinctorum)* Biomass was shown by Burevska [15] and Gratia [16] to be particularly promising with peanut husk powder yielding the most desirable result at pH 6.5 and biosorbent dosage of 2.5g/L. However, batch experiments suggests that Lichen Biomass is rather effective at pH 7 with an adsorption capacity recorded at 33.92 mg/g. Komarabathina [17] reported that Liagora viscida algae exhibited a maximum Ni (II) adsorption of 22.77mg/g at pH of 5.

The success of the process is usually depicted in terms of adsorption capacity which measures the overall potential of the adsorbent to adsorb specific contaminants and the removal efficiency which estimates the percentage removal of contaminants per gram of adsorbent under given physico-chemical conditions. Of equal significance is the formulation of kinetic models that enable the examination of the adsorption rates of contaminants onto the surfaces of these adsorbents under diverse physico-chemical conditions. Estimation of kinetic rate constants of a specific adsorbate-adsorbent complex is also essential for potential process scale-up. The precise estimation of the adsorption rate constant holds considerable significance in shaping the design of adsorption systems intended for large-scale or industrial utilization. As noted by Hubbe [18] shortening the time required to achieve equilibrium adsorption can lead to a reduction in system residence time, consequently diminishing the equipment size necessary for treatment. Consequently, this study aims to explore the adsorption kinetics of Ni (II) removal using Palm Kernel Chaff across a spectrum of physico-chemical conditions.

2.0 METHODOLOGY

The carbonized and uncarbonized palm kernel chaff (PKC) utilized in this study were prepared as described by Nnaji et al. [19]. The adsorption of nickel from water-based solutions was investigated employing the completely mixed batch reactor (CMBR) method. Analytical grade Nickel (II) Sulphate solution was procured from Zayo-Sigma Chemicals Limited, Yakubu Gowon Way, Opposite Nasco, Jos, Plateau State. One hundred milligrams of the adsorbent sample A which is described as carbonized Palm Kernel Chaff (CPKC) was added to 100 mL of Nickel (II) sulfate solution at varying concentrations of 10, 30, 50, 70, 100, and 120 mg/L. A constant temperature magnetic stirrer was used to stir samples at temperatures of 30^{o}C, 35^{o}C and 40^{o}C and at a measured starting pH of 3 and 9 respectively. In the same way, 100mg of adsorbent sample B henceforth assigned the label of uncarbonized Palm Kernel Chaff (UCPKC) was added to 100ml of the metal solution at concentrations of 10, 30, 50, 70, 100, and 120mg/l respectively. A constant temperature magnetic stirrer was used to stir samples at temperatures of 30^{o}C, 35^{o}C and 40^{o}C and pH of 3 and 9 respectively. pH was measured using a standard pH meter. This was adjusted using a 0.5M HCl solution to achieve pH 3 and a dilute NaOH solution to attain pH 9. The adsorption experiment was replicated across the identical range of nickel concentrations at both pH 3 and pH 9, and carried out at temperatures of 40°C, 35°C, and 30°C for the Carbonized Palm Kernel Chaff (CPKC) and uncarbonized Palm Kernel Chaff (UCPKC).

To acquire further understanding into the performance, rate, and adsorption mechanism of Ni (II) onto Carbonized Palm Kernel Chaff (CPKC) and uncarbonized Palm Kernel Chaff (UCPKC), it is

necessary to conduct adsorption kinetic studies, as previously demonstrated by Wang and Guo [20]. The examination of adsorption kinetics for CPKC and UCPKC involved sampling from the batch reactors at defined time periods of 5, 10, 20, 30, 40, 60, 90, and 120 minutes for each batch with a fixed initial Ni (II) concentration. Separation of the adsorbent from the solution was achieved through filtration using Whitman filter paper (0.45 µm). Subsequently, metal analysis was performed with an Atomic Absorption Spectroscopy Machine (Shimadzu, AA 7000) on the extracted adsorbate.

The batch experimental adsorption data, involving various initial concentrations and time intervals, were fitted to distinct kinetic models as described in Table 1. These models were formulated to address one of the four fundamental and sequential steps involved in the adsorption of solutes onto sites with reactivity on the adsorbent's surface. These steps encompass (i) the transport of the solute within the main liquid solution, (ii) the propagation of the solute all over the aqueous solution around the adsorbent particle, (iii) the spread of the solute through the liquid within the adsorbent's pores and pore walls (intraparticle diffusion), and (iv) the adsorption and desorption of the solute onto active sites on the adsorbent's layers, as established by [21] in 2013. In a continuously mixed (stirred) system, the first step is mechanically achieved and is therefore excluded from the process.

3.0 RESULTS AND DISCUSSION

3.1 Efficiency of Adsorption of Nickel by Palm Kernel Chaff

With established conditions at pH of 3 and a temperature reading of 30°C, Carbonized Palm Kernel Chaff (CPKC) demonstrated increased adsorption efficiency as the starting concentration of Ni (II) decreased. The efficiency spanned from 14.1% after 5 minutes for an initial concentration of 10 mg/L to 49.2% after 90 minutes for the same initial concentration. For other initial concentrations (30, 50, 70, 100, and 120 mg/L), the adsorption efficiency initially exhibited relatively high performance but was eventually surpassed by the batch with a 10 mg/L initial concentration after approximately 25 minutes, as depicted in Figure 1. Conversely, under the same conditions, including CPKC and a temperature of 30°C but at a pH of 9, the adsorption efficiencies for various initial concentrations significantly exceeded those recorded at pH 3. The efficiency of adsorption ranged from 78.3% after 5 minutes for a starting concentration of 120 mg/L to 97.8% after 60 minutes for an initial concentration of 10 mg/L. Remarkably, the process proceeded so rapidly that within the first five minutes, adsorption efficiencies of 92.3%, 91.1%, 88.6%, 83.5%, 81.4%, and 78.3% were recorded for initial concentrations of 10, 30, 50, 70, 90, 100, and 120 mg/L, respectively. Equilibrium was mostly achieved between 60 and 90 minutes, with an upper limit of 120 minutes.

Table 1: Details of kinetic models used

Model	Native Form	Integrated/Linearized Form	Rate constant	Predicted equilibrium concentration	Remark
PFO	$\frac{dq_t}{dt} = k_1(q_e - q_t)^2$	$Ln(q_e - q_t) = -k_1 t + Lnq_e$ [plot $Ln(q_e - q_t)$ vs t]	$k_1(min^{-1}) = -\text{slope}$	$q_e(mg.g^{-1}) = exp(intercept)$	Unstable as the process approaches equilibrium
IPD	$q_t = f(t^{1/2})$	$q_t = k_p\sqrt{t} + I_d$ [plot q_t vs $\sqrt{t}$]	$k_p(\text{mg } g^{-1}min^{-1}) = slope$	----	
PSO_1	$\frac{dq_t}{dt} = k_2(q_e - q_t)^2$	$\frac{t}{q_t} = \left(\frac{1}{q_e}\right)t + \frac{1}{k_2 q_e^2}$ [plot $\frac{t}{q_t}$ vs t]	$k_2(\text{g } mg^{-1}min^{-1}) = \frac{1}{intercept \times (q_e)^2}$	$q_e(mg.g^{-1}) = \frac{1}{slope}$	Stable
PSO_2		$\frac{1}{q_t} = \left(\frac{1}{k_2 q_e^2}\right)\frac{1}{t} + \frac{1}{q_e}$ [plot $\frac{1}{q_t}$ vs $\frac{1}{t}$]	$k_2(\text{g } mg^{-1}min^{-1}) = \frac{1}{slope \times (q_e)^2}$	$q_e(mg.g^{-1}) = \frac{1}{intercept}$	Unstable at very small values of t
PSO_3		$q_t = \left(-\frac{1}{k_2 q_e}\right)\frac{q_t}{t} + q_e$ [plot q_t vs $\frac{q_t}{t}$]	$k_2(\text{g } mg^{-1}min^{-1}) = -\frac{1}{slope \times q_e}$	$q_e(mg.g^{-1}) = intercept$	Stable
PSO_4		$\frac{q_t}{t} = (-k_2 q_e)q_t + k_2 q_e^2$ [plot $\frac{q_t}{t}$ vs q_t]	$k_2(\text{g } mg^{-1}min^{-1}) = -\frac{slope}{q_e}$	$q_e(mg.g^{-1}) = \sqrt{\frac{intercept}{k_2}}$	Stable
PSO_5		$\frac{1}{t} = k_2 q_e^2\left(\frac{1}{q_t}\right) - k_2 q_e$ [plot $\frac{1}{t}$ vs $\frac{1}{q_t}$]	$k_2(\text{g } mg^{-1}min^{-1}) = \frac{slope}{(q_e)^2}$	$q_e(mg.g^{-1}) = -\frac{intercept}{k_2}$	Unstable at very small values of t
PSO_6		$\frac{1}{(q_e - q_t)} = k_2 t + \frac{1}{q_e}$ [plot $\frac{1}{(q_e - q_t)}$ vs t]	$k_2(\text{g } mg^{-1}min^{-1}) = slope$	$q_e(mg.g^{-1}) = \frac{1}{intercept}$	Unstable as the process approaches equilibrium

Additionally, it was observed that the batch with an initial Ni (II) amount of 10 mg/L initially lagged but gradually gained an advantage after approximately 25 minutes, ultimately surpassing all other batches after about 40 minutes of contact time. Under the same conditions (CPKC, at a temperature of 35°C and pH), the adsorption performance ranged from 79.6% after 5 minutes for a starting concentration of 120 mg/L to 97% after 90 minutes for an initial concentration of 10 mg/L. Although the batch with a starting concentration of 10 mg/L exhibited higher adsorption efficiencies, it could not maintain this lead, unlike the results at 30°C. After an initial 30-minute advantage, the batch with an amount of Ni (II) at 30 mg/L made substantial gains, surpassing it at approximately 75 minutes of contact time.

When CPKC had a temperature of 40°C at a pH of 3, a similar trend was observed, analogous to other pH 3 conditions. The performance for a starting concentration of 10 mg/L lagged other batches until around 25 minutes, after which it began to improve over some other batches and eventually took the lead after about 35 minutes. The adsorption efficiency ranged from 28.7% after 5 minutes for a concentration amount of 10 mg/L to 66.9% after 90 minutes for the same initial concentration. Upon closer examination, an increase in the temperature of the aqueous solution from 30°C to 40°C resulted in a doubling of the adsorption efficiency within the first 10 minutes of contact time for low to medium starting Ni (II) concentrations (10–50 mg/L). This indicates that temperature enhancement facilitates a faster initiation of the process, thereby diminishing the timeframe needed to attain equilibrium-stability. To underscore this effect, 44% of Ni (II) was withdrawn from the solution at only 5 minutes when conditions were at 40°C, while it took approximately 30 minutes and over 120 minutes to achieve a similar percentage removal at 35°C and 30°C, respectively.

The same trend as observed for the carbonized adsorbent was also observed for the uncarbonized adsorbent (UCPKC) to varying degrees (Figure 2). The adsorption rate of Ni (II) at pH 3 on the non-carbonized adsorbent was observed to be slower than that onto the carbonized adsorbent. Specifically, the efficiency of adsorption of Ni (II) onto uncarbonized Palm Kernel Chaff (UCPKC) under pH 3 conditions at 30°C ranged from 3.1% after 5 minutes for a starting amount of 10 mg/L which is about 5 times lower than what was recorded for the CPKC to 48.8% after 90 minutes which is just 0.4% below what was recorded for CPKC within the same time frame. Hence, it does appear that the advantage of carbonization in this case is to enhance the initial stages of Ni (II) adsorption onto PKC, but with no long-term positive effect except for marginal gain in adsorption efficiency. Nonetheless, the disparity in performance between the two materials becomes more pronounced with rising temperatures. At 35°C, the equilibrium adsorption percentages for UCPKC at pH 3 were measured at 49.9%, 45.6%, 39.2%, 38.1%, 34.2%, and 33.9% for initial concentrations of 10, 30, 50, 70, 100, and 120 mg/L, respectively. In comparison, the corresponding adsorption efficiencies for CPKC under the same pH and temperature conditions were notably higher, at 59.3%, 49.2%, 49.5%, 47.7%, 40%, and 38.4%. This indicates that carbonization not only accelerates the rate of adsorption but also elevates the adsorption capacity of Palm Kernel Chaff (PKC) for Ni (II) by as much as 10% when operating at a temperature of 35°C.

It is worth noting that while increasing the operating temperature to 40°C leads to a further improvement in the rate of adsorption, it does not yield the same degree of increase in the adsorption capacity of the carbonized adsorbent over the non-carbonized one. When pH was set at 3 and temperature at 40°C, the equilibrium adsorption efficiencies for UCPKC were observed to be 62.4%, 52.5%, 50.8%, 49.2%, 45.7%, and 42.6% for initial concentrations of 10, 30, 50, 70, 100, and 120 mg/L, respectively. The corresponding values for CPKC were 66.9%, 58.2%, 55.6%, 50.2%, 47.4%, and 44.6%. It is evident that the highest improvement in equilibrium adsorption percentage at a temperature of 40°C is 5.7%. Upon closer examination, it becomes obvious that temperature undertakes a significant role in the uptake of Ni (II) onto PKC. For example, a 5°C temperature increase from 35°C to 40°C results in a percentage range of equilibrium adsorption efficiency improvement of 6.9 to 13.3 at pH 3 for UCPKC and 6.5 to 9.0 for CPKC. The same observation also applies to the impact of pH.

Under pH 9 conditions at 30°C, the adsorption efficiency for UCPKC ranged from 61.8% after 5 minutes for a concentration starting at 120 mg/L to 88.9%, after 90 minutes, for a starting concentration amount of 10 mg/L. These values were significantly higher than those recorded at pH 3, which stood at 3.1% and 48.8%, respectively. As further illustrated in Figure 3, pH takes on a substantial function in the uptake of Ni (II) onto PKC. CPKC displayed superior performance in alkaline solutions (pH 9) compared to acidic ones (pH 3), with multiplicative factors ranging from 2.0 to 2.6 at 30°C, 1.6 to 2.2 at 35°C, and 1.5 to 1.9 at 45°C at equilibrium for the entire span of starting concentrations investigated. For UCPKC, the

corresponding factors were 1.8 to 2.6, 1.9 to 2.0, and 1.6 to 1.8. These results indicate that PKC, whether carbonized or not, performs approximately two times better at pH 9 than at pH 3. The difference in performance between the two pH conditions is even more pronounced at the onset of adsorption, where the efficiency of Ni(II) removal after 5 minutes at pH 9 exceeded that at pH 3 by a factor of 6.5 for CPKC at 30°C. Figure 3 further illustrates that an increase in temperature tends to narrow the efficiency gap in the uptake of Ni (II) onto PKC by enhancing the process's effectiveness at pH 3. This is further supported by the general decrease in the ratio of the quantity of Ni(II) taken off when the pH is at 9 to that when the pH is at 3. Consequently, the most favorable results were obtained at pH 9 and at 40°C temperature for the entire range of initial concentrations studied, with equilibrium adsorption efficiencies ranging from 84.9% for a 120 mg/L starting concentration after 90 minutes of contact time to 99.99% for a starting Ni (II) amount of 10 mg/L at 60 minutes.

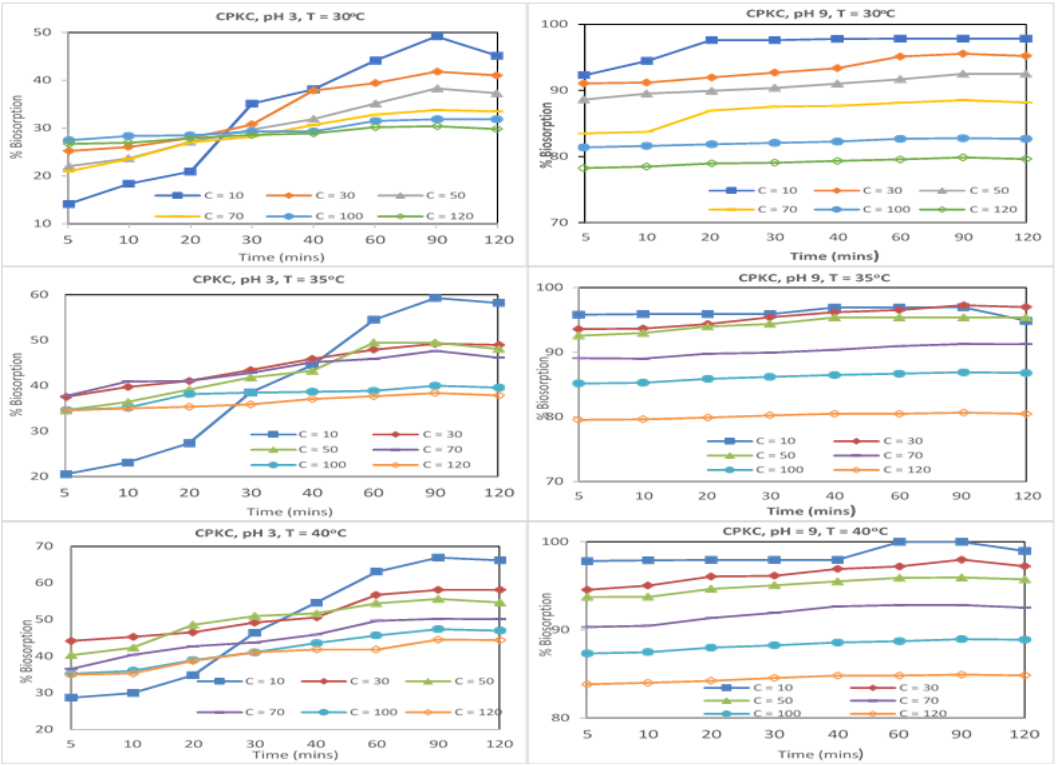

Figure 1: Efficiency of carbonized PKC for Nickel Adsorption

To further illustrate the higher efficiency of Ni (II) adsorption onto PKC at pH 9 compared to pH 3, we can consider the pH point-zero charges (pHpzc) of the two materials. The pHpzc values for CPKC and UCPKC, which indicate the pH where the materials have a net surface field charge of zero, were determined to be 4.1 and 4.6, respectively. The figures clearly suggests that the materials assume a net positive field charge in an acidic medium and a net negative field charge when the medium is alkaline in nature. Given that Ni (II) is a positively charged ion, it has a greater affinity for the adsorbent that carries a net negative charge in an aqueous solution, precisely the scenario when the adsorbents encounter the adsorbate solution maintained at pH 9. The pHpzc values also suggest that carbonization further enhances the adsorption capacity of PKC by reducing the pHpzc value, thereby creating a stronger affinity between the solute and the adsorbent. This electrostatic repulsion at low pH accounts for the reduced performance of PKC at pH 3. Furthermore, increase in pH enhances deprotonation of the functional groups on the surface of the palm kernel chaff, thereby creating more negatively charged sites and increasing the performance of the adsorbent at pH9. This explains why CPKC outperforms UCPKC in terms of adsorption efficiency under the same physico-chemical conditions [19]. Additionally, previous studies have reported higher efficiencies for the adsorption of Nickel at higher pH values compared to lower ones. In a comprehensive review of Ni (II) adsorption, Islam [22] reported that most of the studies reviewed, there was no suggestion of adsorption of Ni (II) at low pH. Furthermore, Nirmala [23], who investigated the uptake of Ni(II) onto Andrographis Paniculata leaves, explained that at low pH, the

adsorbent surface acquires a net positive field charge, resulting in electrostatic rejection between the adsorbate and the adsorbent.

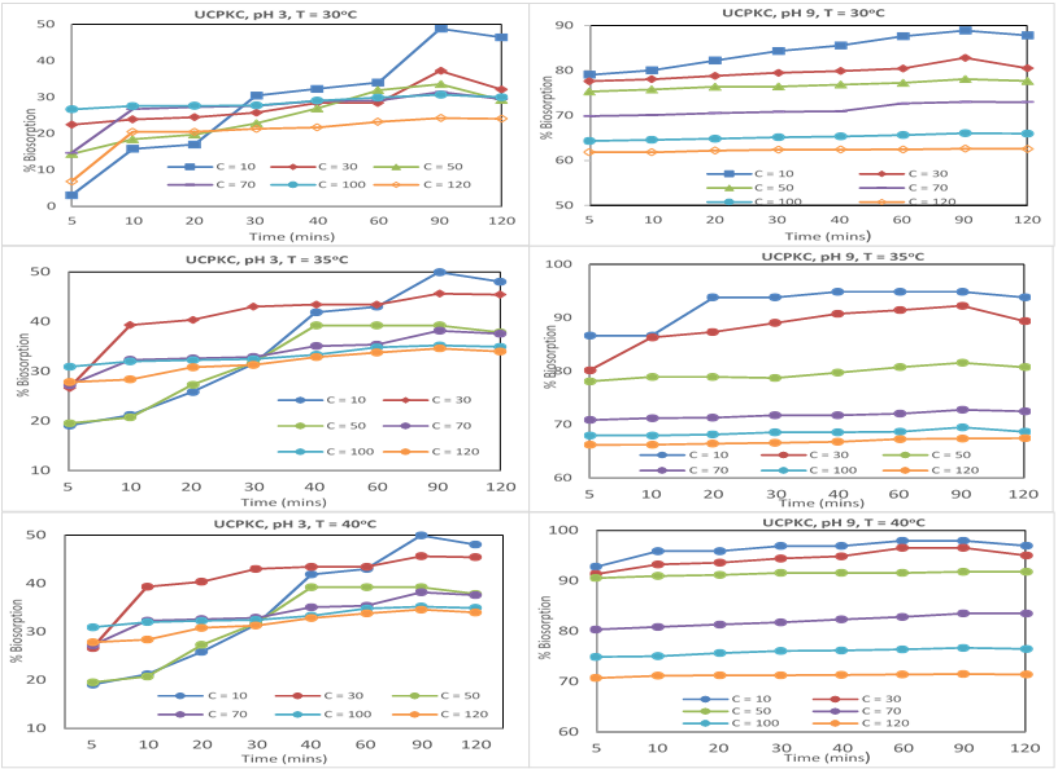

Figure 2: Efficiency of uncarbonized PKC for Nickel Adsorption

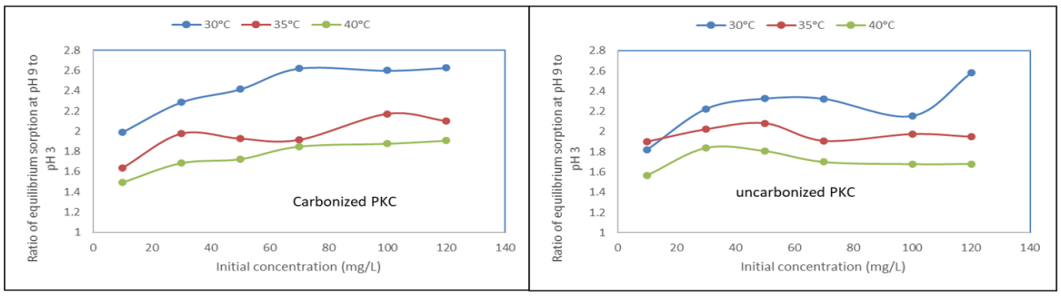

Figure 3: Effect of pH on comparative performance of CPKC and UCPKC

As observed for CPKC, the uptake of Ni (II) onto PKC exhibits a slow start at low initial concentrations (10 mg/L). Consequently, its performance initially lags batches with higher initial concentrations but quickly gains momentum and begins to surpass them just after 20 minutes of contact time. By the thirtieth minute, it had exceeded all the others when the adsorption performance is considered. However, Figure 2 illustrates that when the adsorption temperature is raised to 35°C and 40°C, the batch with a starting concentration of 30 mg/L maintains its superior performance over that of 10 mg/L until after 60 minutes. Furthermore, the performances of UCPKC at pH 3 for the various initial concentrations studied are quite close and even indistinguishable at some points compared to pH 9, which exhibits very distinct and distinguishable plots for the various initial concentrations.

Nnaji [19] reported that considering the range of adsorption conditions for the uptake of Nickel (II) by PKC, the adsorption capacity of the material at high adsorbate concentrations is best described by the Langmuir linear type II isotherm ($0.96 \leq R2 \leq 1.0$) compared to the non-linear isotherm. This is because the Langmuir (II) isotherm had the highest R^2 values and low error margins. It was noted that applying an ion exchange monolayer coverage, the adsorbent dose of one gram (1 g) had the potential to completely remove up to 120.6 mg of Nickel from an aqueous solution at optimal study conditions at pH 9 and 35°C. In addition, CPKC with a maximum adsorption

capacity (q_{max}) of 65.4 to 120.6 mg/g performed better than UCPKC with q_{max} of 36.0 to 65.9 mg/g. The value of the adsorption energy given as $8.21 \leq E \leq 14.27$ and the isosteric heat of adsorption given as $-133.09 \leq \Delta Hx \leq -17.92$ indicates a mode of adsorption which is mostly driven by ionic exchange.

3.2 Kinetics of Ni (II) Adsorption Onto CPKC And UCPKC

The rate constants obtained from resolving the kinetic equations varied according to the prevailing physico-chemical conditions during the batch adsorption process. In the case of CPKC, when the initial pH was measured as 3 and the temperature was set at 30°C, the rate constants estimated using the PFO, IPD and various forms of PSO kinetic models typically exhibited an upward trend when the starting concentration was 10 mg/L which progressively increased to higher rate constant values when the starting concentration was increased to 30 mg/L. This however was not the case for PSO_6. Subsequently, the rate constants experienced a slight decrease until they began increasing again at starting concentration of 70 mg/L.

The PSO_6 and intraparticle diffusion (IPD) models displayed slight differences in behavior. The PSO_6 rate constants decreased from 0.3 g/mg·min^{-1} at an initial amount of Ni (II) at10 mg/L to 0.09 g/mg·min^{-1} at a starting concentration of 50 mg/L, after which they rapidly increased to 0.59 g/mg·min^{-1} at a starting Ni (II) concentration of 120 mg/L. Conversely, the IPD kinetic model demonstrated a contrasting pattern, with rate constants increasing from 0.06 g/mg·min^{-1} at an initial concentration of 10 mg/L to 0.13 g/mg·min^{-1} at a starting concentration of 70 mg/L, before eventually dropping to 0.07 g/mg·min^{-1} at an initial amount of 120 mg/L. The pseudo-second order kinetic models generally yielded higher rate constants at pH 9 than at pH 3 across all temperatures. For CPKC at pH 3 and a temperature of 30°C, the rate constants for PSO_1, PSO_2, PSO_3, PSO_4, PSO_5, and PSO_6 ranged from 0.06 to 0.16, 0.14 to 0.44, 0.13 to 0.42, 0.13 to 0.30, and 0.09 to 0.59 g/mg·min^{-1} across various batches with varying starting Ni (II) concentrations. The corresponding rate constants at pH 9 were notably higher, ranging from 0.33 to 2.8, 0.48 to 2.92, 0.47 to 2.92, 0.40 to 2.79, and 0.4 to 2.79 g/mg·min^{-1}. For UCPKC with pH set at 3 and a temperature of 30°C, the rate constants for PSO_1, PSO_2, PSO_3, PSO_4, PSO_5, and PSO_6 fell within the range of 0.01 to 0.16, 0.01 to 0.58, 0.07 to 0.51, 0.01 to 0.31, 0.01 to 0.33, and 0.03 to 0.18 g/mg·min^{-1}, which were generally lower than the corresponding values at pH 9, ranging from 0.28 to 1.14, 0.95 to 1.94, 0.9 to 1.94, 0.91 to 1.57, 0.55 to 1.57, and 0.14 to 1.16 g/mg·min^-1. This further confirms the patterns previously observed in the adsorption efficiency results discussed earlier, indicating that a boost in solution pH from 3 to 9 enhances the rate of Ni (II) removal from aqueous solution using PKC.

In nearly all cases, PSO_1 models outperformed others, as indicated by the R-squared (R^2) values, which spanned from 0.8 to 1.0, respectively, followed by the IDP ($0.56 < R^2 < 1.0$) and PFO ($0.65 < R^2 < 0.99$) for CPKC and UCPKC at a temperature of 30°C for both pH 3 and 9. The lower values of R^2 were observed in the UCPKC batch for pH 3. This suggests that the process of sorption of Ni (II) onto PKC is characterized by both a sluggish pace and lower efficiency at pH 3. which is not totally amenable to description using any of the regular kinetic models used in this study. PSO_4, PSO_5 and PSO_6 are the least performing of the kinetic models. There are still pockets of points where these models performed acceptably but overall, they were largely inconsistent in generally describing the kinetics of Ni (II) adsorption onto PKC. This suggests that the PSO_1 is superior to other variants of PSO that resulted from mathematical manipulations of PSO_1 for the adsorption of Ni (II) onto PKC and is therefore not justified. The same trend is also clearly noticeable for CPKC and UCPKC for both pH 3 and 9 at a temperature of 35°C with PSO_1 yielding the highest R^2 values (0.91 – 1.0), followed by PFO ($0.7 < R^2 < 1.0$) and IPD ($0.64 < R^2 < 1.0$). PSO_6 also gave lower but still reasonably good R^2 values ($0.63 < R^2 < 0.99$) with the other kinetic models performing less. The same trend was also observed at 40°C for both CPKC and UCPKC with PSO_1 consistently yielding the highest R^2 ($0.92 < R^2 < 0.99$), followed by PFO ($0.67 < R^2 < 0.98$) and IPD ($0.63 < R^2 < 9.8$).

The PSO_1 kinetic rate constants generally increased with increase in temperature but the pattern of behavior for pH is not consistent enough to be generalized. There was a general increase in rate of adsorption from pH 3 to pH 9 for batches investigated at 30°C and 40°C but the reverse was the case for 35°C (Figures 4 – 6). The PSO_1 kinetic rate constants for 35°C ranged from 0.57 – 0.85 g/mg.min^{-1} when the pH was set at 3 and 0.02 – 0.7 g/mg.min^{-1} when the pH was at 9 for CPKC (Figure 5). In the same manner, the PSO_1 rate constant ranged from 0.39 – 1.29 g/mg.min^{-1} at a pH of 3 and 0.23 – 0.36 g/mg.min^{-1} at a pH of 9 for UCPKC. One can infer from these values that the rate of uptake of Ni (II) onto PKC occurs at a faster rate at pH 3 when compared to pH 9 with a temperature set at 35°C.

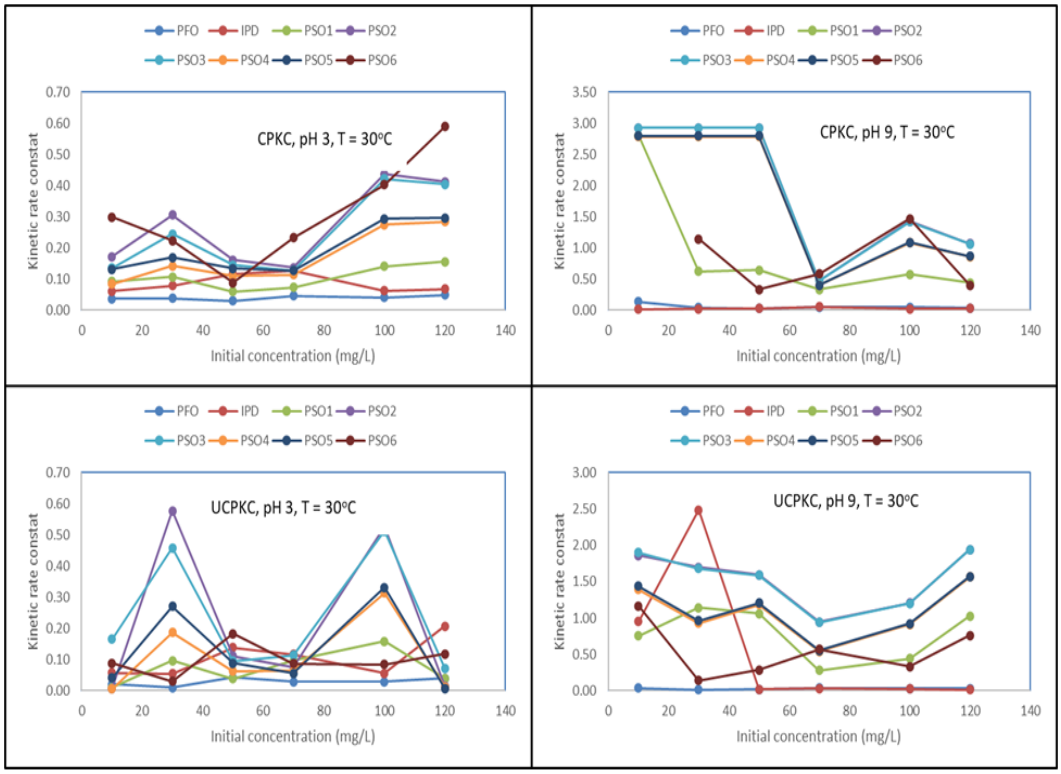

Figure 4: Kinetic rate constants of Nickel sorption by carbonized and uncarbonized PKC at 30°C

The kinetic rate constants at 30°C ranged from 0.06 – 0.16 g/mg.min^{-1} at pH 3 and 0.33 – 2.80 g/mg.min^{-1} at pH 9 for CPKC; and 0.01 – 0.16 g/mg.min^{-1} at pH 3 and 0.44 – 1.14 g/mg.min^{-1} at pH 9 for UCPKC (Figure 4). The PSO_1 rate constant for CPKC at 40°C ranged from 0.64 – 5.42 g/mg.min^{-1} at pH 3 and 0.98 – 10.20 g/mg.min^{-1} at pH 9. The corresponding rate coefficient for UCPKC at the same temperature ranged from 0.67 - 5.13 g/mg.min^{-1} and 0.98 – 8.58 g/mg.min^{-1}. The greatest difference in adsorption rate between batch processes conducted at pH 3 and that conducted at pH 9 was observed at lower temperatures (30°C) with the rate constants obtained at pH 3 exceeding that recorded when the pH was 9. This is nearly nine times for CPKC and 11 times for UCPKC. As the temperature increased to 40°C, this disparity in adsorption rate constants dropped sharply to about two and five times for CPKC and UCPKC respectively. This clearly shows that increase in temperature can compensate for difference in pH during the adsorption. The average increase in adsorption rate constant for CPKC (pH 3), CPKC (pH 9), UCPKC (pH 3) and UCPKC for 1°C increase in temperature was 0.31, 0.98, 0.51 and 0.43 g/mg.min^{-1} respectively. A close examination of the results also suggests that the rate of uptake of Ni (II) to PKC is faster for carbonized than the uncarbonized PKC at 30°C and 40°C. It has been explained before that chemisorption mechanism cannot be established by the good fit of PSO. However, the remarkable effect of temperature on the adsorption process might confirm a chemisorption mechanism. It has been reported that chemisorption is at play when the rate constant is dependent on solute concentration and temperature [24].

3.3 Comparative Performance of Kinetic Models by Applying Average Relative Error (ARE)

Based on the best performing kinetic model (PSO_1), the rate of adsorption of Ni (II) to PKC can be further probed into for different physico-chemical conditions. Though it has earlier been noted that PSO_1 was the most appropriate for describing the kinetics of Ni (II) adsorption onto PKC based on R^2 values, it is important to subject the models to further scrutiny to establish more concretely which models are best suited to describe the process or not in terms of adsorption rate. This is because a high coincidental association between two variables can yield high values of R^2 even when the change in one variable does not sufficiently explain change in the dependent variable. Besides, [25] affirms that though PSO_1 has been generally reported to give very good fits to experimental adsorption data due to the high R^2 values, it should be applied with caution because it sometimes gives poor estimates of the equilibrium concentration (q_e) and the adsorption rate constant (k).

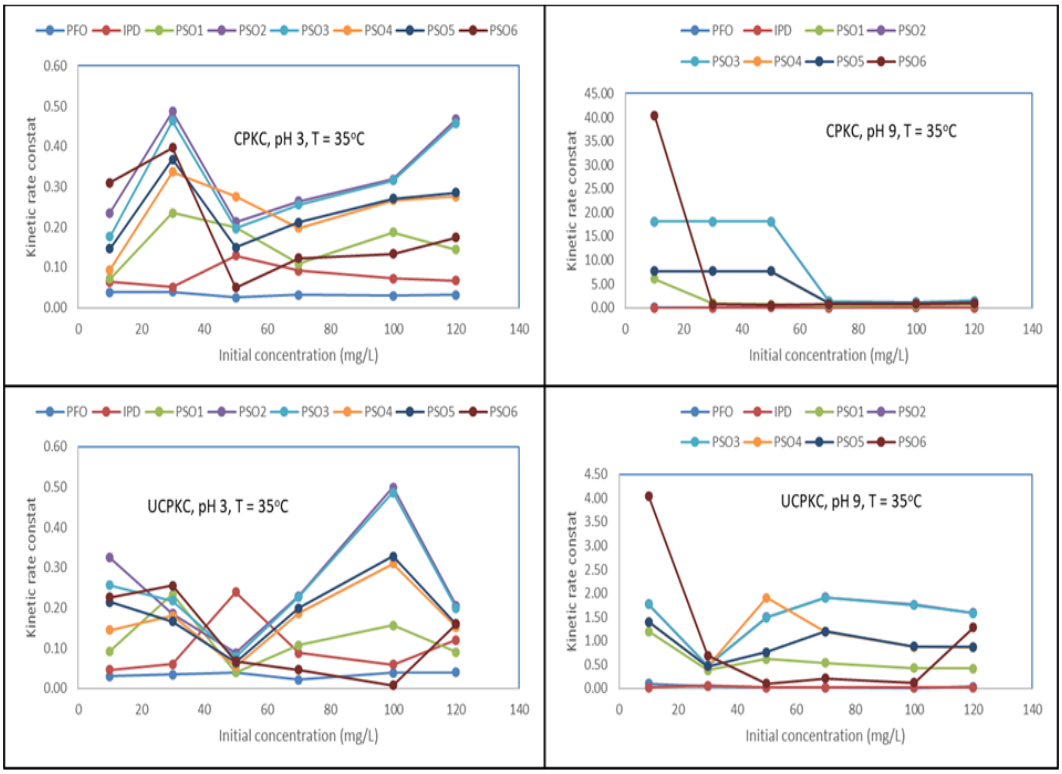

Figure 5: Kinetic rate constants of Nickel sorption by carbonized and uncarbonized PKC at 35°C

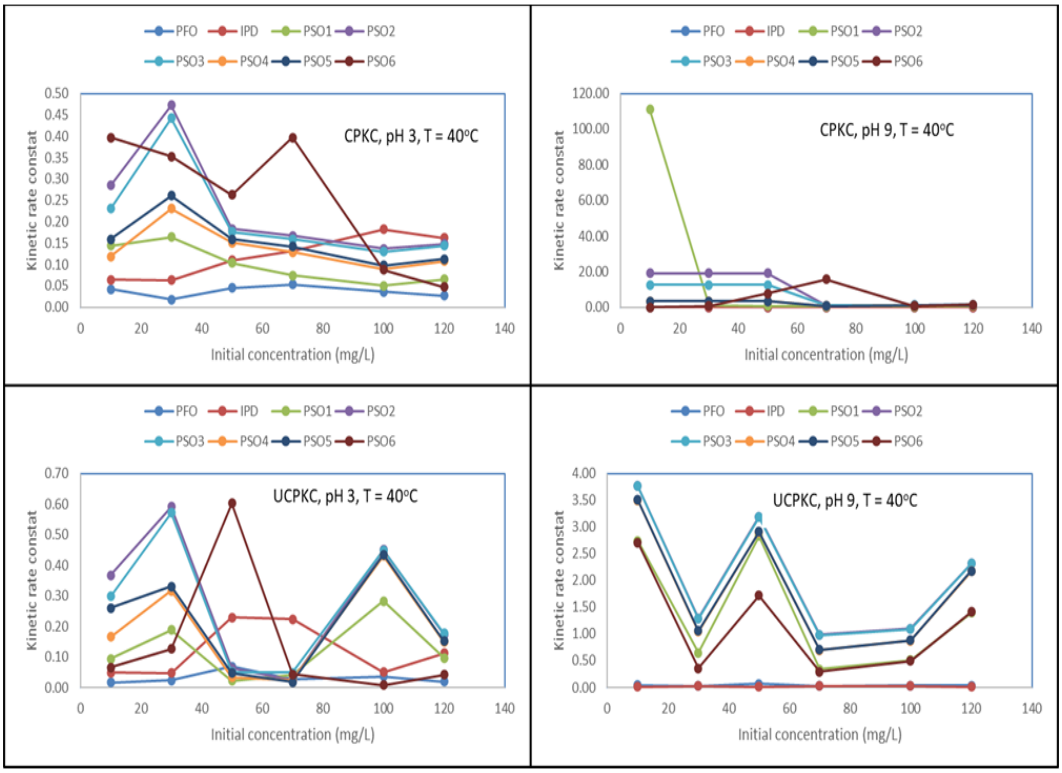

Figure 6: Kinetic rate constants of Nickel sorption by carbonized and uncarbonized PKC at 40°C

Based on average relative error, PFO and PSO_6 performed relatively poorly at all temperature and pH. The average relative error (ARE) for PFO ranged from 0.5 – 0.94, 0.61 – 0.92 and 0.62 – 0.97 at 30°C, 35°C and 40°C while the corresponding values for PSO_6 ranged from 0.99 – 1.77, 0.75 – 1.42 and 0.73 – 1.24. Again, PSO_1 still proved to be a more reliable model for describing the kinetics of uptake of Ni (II) to PKC. The ARE of PSO_1 ranged from 0.0041 – 0.24, 0.0024 – 0.048 and 0.0022 – 0.052 at 30°C, 35°C and 40°C.

Plazinski [21] opined that the PFO and PSO assume that rate of transfer of solute particles located within the vicinity of the adsorbent active sites onto the adsorbent active sites which play a pivotal role, either dictate the entirety of the process or participate partially in the process. However, this position cannot reasonably and convincingly explain why both models seem to fit a wide range of experimental adsorption data. It appears however that the high correlation exhibited by these two models when applied to adsorption data is due to the structure of the models which suggests that adsorption rate is proportional to $(q_e - q_t)$ and represents the driving force from the bulk liquid phase to the adsorption site. In essence, both PFO and PSO tend to consider the adsorption process as a single-step process rather than a multi-stage process. Hence, they tend to aggregate the differential rates of the various steps into a singular representative rate constant (k_1 or k_2) thus implying that the last stage (adsorption-desorption onto active sites) is the rate-defining step. The structure of the IPD kinetic model when plotted to the data ($I_p \neq 0$) suggests that the adsorption of Ni (II) onto CPKC and UCPKC is a multiple adsorption system [19], though intraparticle diffusion tend to dominate in the batch adsorption experiment conducted at 30°C and low NI (II) concentrations of 10 mg/L.

From the foregoing, the kinetic models can be grouped as follows in terms of performance based on ARE: /PSO1/ > /PFO/ > /PSO2-5/ > /PSO6/. Numerous prior studies have documented that the pseudo-second-order kinetic model provided the most favorable fit for a diverse spectrum of adsorbents and adsorbates, including fly ash and Congo Red dye [9], Pea peel and acid yellow dye [8], coconut shell and methylene blue [26], Rosa Damascene leaves and copper [7], and walnut and Chromium [27]. It may be noted that PSO kinetic model was able to fit these experimental adsorption data though the adsorbent-adsorbate combination differed widely. Plazinski [21] adduced that the good performance of PSO kinetic model in describing most adsorption processes reported in the literature could be either due to similarity in the adsorption mechanisms of the adsorbent-adsorbate system investigated or the flexibility of the mathematical forms of the model are valid for a wide range of adsorbent-adsorbate interactions.

4.0 CONCLUSION

The investigations show the effect of important batch variables on the efficiency and kinetics of adsorption of Ni (II) onto Carbonized (CPKC) and uncarbonized (UCPKC) Palm Kernel Chaff. Adsorption equilibrium was attained at 60 – 120 minutes for all samples while improved adsorption efficiencies were observed at pH 9 compared to pH 3. In addition, rapid adsorption was noted within the first 5 minutes with efficiencies ranging from 78.3% at 5 minutes and starting concentration of 120 mg/L and 97.8% at 60 minutes for an initial concentration amount of 10 mg/L. Adsorption efficiency and capacity was improved by carbonization by up to 10% at an operating temperature of 35°C. In nearly all cases, PSO_1 model performed better than other kinetic models with R^2 values ranging from 0.8 to 1.0. The average increase in adsorption rate constant for CPKC (pH 3), CPKC (pH 9), UCPKC (pH 3) and UCPKC for 1°C increase in temperature was 0.31, 0.98, 0.51 and 0.43 g/mg.min-1 respectively. Based on the average relative error estimates (ARE), the kinetic models can be grouped as follows in terms of performance: /PSO1/ > /PFO/ > /PSO2-5/ > /PSO6/.

REFERENCES

[1] IPCS, "Nickel," Geneva, 1991. Accessed: Jan. 05, 2024. Available: https://www.inchem.org/documents/ehc/ehc/ehc108.htm

[2] WHO, "Nickel in drinking-water," 2021. Available: http://apps.who.int/bookorders.

[3] G. Genchi, A. Carocci, G. Lauria, M. S. Sinicropi, and A. Catalano, "Nickel: Human Health and Environmental Toxicology," *International Journal of Environmental Research and Public*, vol. 17, no. 3, p. 679, 2020, doi: 10.3390/ijerph17030679.

[4] C. T. Matos *et al.*, "Material System Analysis of five battery related raw materials: Cobalt, Lithium, Manganese, Natural Graphite, Nickel," Luxembourg, 2020. doi: 10.2760/519827.

[5] Y. Ojima, S. Kosako, M. Kihara, N. Miyoshi, K. Igarashi, and M. Azuma, "Recovering metals from aqueous solutions by biosorption onto phosphorylated dry baker's yeast," *Scientific Reports*, vol. 9, no. 1, 2019, doi: 10.1038/s41598-018-36306-2.

[6] X. Guo and J. Wang, "Comparison of linearization methods for modeling the Langmuir adsorption isotherm," *Journal of Molecular Liquids*, vol. 296, p. 111850, 2019, doi: https://doi.org/10.1016/j.molliq.2019.111850.

[7] Fawzy, M. A., Al-Yasi, H. M., Galal, T. M., Hamza, R. Z., Abdelkader, T. G., Ali, E. F., & Hassan, S. H. A. "Statistical optimization, kinetic, equilibrium isotherm and thermodinamic studies of copper biosorption onto Rosa damascena leaves as a low-cost biosorbent",

Scientific Reports, vol 12, no. 1. 2022; https://doi.org/10.1038/s41598-022-12233-

[8] M. A. El-Nemr, M. Yılmaz, S. Ragab, M. A. Hassaan, and A. El Nemr, "Isotherm and kinetic studies of acid yellow 11 dye adsorption from wastewater using Pisum Sativum peels microporous activated carbon," *Scientific Reports*, vol. 13, no. 1, Dec. 2023, doi: 10.1038/s41598-023-31433-x.

[9] M. Harja, G. Buema, and D. Bucur, "Recent advances in removal of Congo Red dye by adsorption using an industrial waste," *Scientific Reports*, vol. 12, no. 1, Dec. 2022, doi: 10.1038/s41598-022-10093-3.

[10] G. Mosoarca, C. Vancea, S. Popa, M. Gheju, and S. Boran, "Syringa vulgaris leaves powder a novel low-cost adsorbent for methylene blue removal: isotherms, kinetics, thermodynamic and optimization by Taguchi method," *Scientific Reports*, vol. 10, no. 1, Dec. 2020, doi: 10.1038/s41598-020-74819-x.

[11] N. U. M. Nizam, M. M. Hanafiah, E. Mahmoudi, A. A. Halim, and A. W. Mohammad, "The removal of anionic and cationic dyes from an aqueous solution using biomass-based activated carbon," *Sciientific Reports*, vol. 11, no. 1, 2021, doi: 10.1038/s41598-021-88084-z.

[12] J. Fito *et al.*, "Adsorption of methylene blue from textile industrial wastewater using activated carbon developed from Rumex abyssinicus plant," *Scientific Reports*, vol. 13, no. 1, Dec. 2023, doi: 10.1038/s41598-023-32341-w.

[13] A. A. Ghoniem *et al.*, "Pseudomonas alcaliphila NEWG-2 as biosorbent agent for methylene blue dye: optimization, equilibrium isotherms, and kinetic processes," *Scientific Reports*, vol. 13, no. 1, Dec. 2023, doi: 10.1038/s41598-023-30462-w.

[14] S. A. Bani-Atta, "Potassium permanganate dye removal from synthetic wastewater using a novel, low-cost adsorbent, modified from the powder of Foeniculum vulgare seeds," *Scientific Reports*, vol. 12, no. 1, Dec. 2022, doi: 10.1038/s41598-022-08543-z.

[15] K. A. Burevska *et al.*, "Biosorption of nickel ions from aqueous solutions by natural and modified peanut husks: equilibrium and kinetics," *Water and Environment Journal*, vol. 32, no. 2, pp. 276–284, May 2018, doi: 10.1111/wej.12325.

[16] Z. K. Gratia, R. Nandhakumar, B. Mahanty, S. Murugan, P. Muthusamy, and K. S. Vinayak, "Biosorption of Nickel from Metal Finishing Effluent Using Lichen Parmotrema tinctorum Biomass," *Water, Air and Soil Pollution*, vol. 232, no. 11, Nov. 2021, doi: 10.1007/s11270-021-05431-6.

[17] S. Komarabathina, K. Pulipati, M. Pujari, and J. Kodavaty, "Biosorption of nickel from aqueous solution onto Liagora viscida: Kinetics, isotherm, and thermodynamics," *Environmental Progress and Sustainable Energy* , 2020, doi: https://doi.org/10.1002/ep.13330.

[18] M. A. Hubbe, S. Azizian, and S. Douven, "Implications of Apparent Pseudo Second-Order Adsorption Kinetics onto Cellulosic Materials: A Review," *Bioresources*, vol. 14, no. 3, pp. 7582–7626, 2019, doi: 10.15376/biores.14.3.7582-7626.

[19] C. C. Nnaji, A. E. Agim, C. N. Mama, P. G. C. Emenike, and N. M. Ogarekpe, "Equilibrium and thermodynamic investigation of biosorption of nickel from water by activated carbon made from palm kernel chaff," *Scientific Reports*, vol. 11, no. 1, 2021, doi: 10.1038/s41598-021-86932-6.

[20] J. Wang and X. Guo, "Adsorption isotherm models: Classification, physical meaning, application and solving method," *Chemosphere*, vol. 258. Nov. 01, 2020. doi: 10.1016/j.chemosphere.2020.127279.

[21] W. Plazinski, J. Dziuba, and W. Rudzinski, "Modeling of sorption kinetics: The pseudo-second order equation and the sorbate intraparticle diffusivity," *Adsorption*, vol. 19, no. 5, pp. 1055–1064, Oct. 2013, doi: 10.1007/s10450-013-9529-0.

[22] M. A. Islam, M. R. Awual, and M. J. Angove, "A review on nickel(II) adsorption in single and binary component systems and future path," *Journal of Environmental Chemical Engineering*, vol. 7, no. 5. Oct. 01, 2019. doi: 10.1016/j.jece.2019.103305.

[23] S. Nirmala, A. Pasupathy, and M. Raja, "Removal Of Nickel (II) Ions From Aqueous Solutions Using Adsorbent Obtained From Andrographis Paniculata Leaves As A Low Cost Adsorbent," *International Journal of Scientific and Research Publications*, vol. 6, no. 11, p. 524, 2016, [Online]. Available: www.ijsrp.org

[24] Y. S. Ho and G. McKay, "Pseudo-second order model for sorption processes," *Process Biochemistry*, vol. 34, no. 5, pp. 451–465, 1999, doi: 10.1016/S0032-9592(98)00112-5.

[25] H. N. Tran, "Applying Linear Forms of Pseudo-Second-Order Kinetic Model for Feasibly Identifying Errors in the Initial Periods of

Time-Dependent Adsorption Datasets," *Water*, vol. 15, no. 6, Mar. 2023, doi: 10.3390/w15061231.

[26] O. Oribayo, O. Olaleye, A. S. Akinyanju, K. O. Omoloja and S. O. Williams, "Coconut Shell-Based Activated Carbon As Adsorbent For The Removal Of Dye From Aqueous Solution: Equilibrium, Kinetics, And Thermodynamic Studies," Nigerian Journal of Technology, vol. 39, no. 4, pp. 1076 - 1084, 2020.

[27] R. Garg *et al.*, "Rapid adsorptive removal of chromium from wastewater using walnut-derived biosorbents," *Scientific Reports*, vol. 13, no. 1, Dec. 2023, doi: 10.1038/s41598-023-33843-3.